Medical Informatics Group

Cardiac Action Potential Prolongation Induced by Isolated Thioridazine Enantiomers

PhD Thesis by
Ask Schou Jensen

River Publishers

Cardiac Action Potential Prolongation Induced by Isolated Thioridazine Enantiomers

Cardiac Action Potential Prolongation Induced by Isolated Thioridazine Enantiomers

PhD Thesis by

Ask Schou Jensen

Medical Informatics Group,
Department of Health Science and Technology,
Aalborg University, Denmark

River Publishers

ISBN: 978-87-93237-42-1 (Ebook)

Published, sold and distributed by:
River Publishers
Niels Jernes Vej 10
9220 Aalborg Ø
Denmark

Tel.: +45369953197
www.riverpublishers.com

Contents

A. Preface and Acknowledgements

This thesis was submitted in partial fulfillment of the PhD degree at the Department of Health Science and Technology, Aalborg University. The thesis is based on three papers written during my enrollment as a PhD student. The work presented would not have been possible without the guidance, support, and opportunities provided by a number of people which must be acknowledged. Several people from outside Aalborg University were instrumental in initiating this project. First of all, I would like to thank Jette Elizabeth Kristiansen associated with the South Danish University for introducing us to thioridazine and creating the opportunity for carrying out this project. I also must thank her for her many kind words along the way. I would also like to thank Jørn Bolstad Christensen at Copenhagen University for his technical expertise which produced the compounds that made the project possible. At Aalborg University, very substantial contributions were made by Cristian Sevcencu and Cristian Pablo Pennisi. I would like to thank both Cristi and Pablo for the great theoretical knowledge, technical expertise, practical experience, and problem solving skills with which they have contributed. Both have showed enormous patience with my incessant questions, and I have greatly enjoyed their support and the sense of understated humor which they share. I would like to thank the entire Cardiotechnology group, but especially I want to thank Samuel Emil Schmidt for the opportunities he made possible and for his infectious optimism and extremely productive intellect. In addition, I have to thank my current and former office mates Kirstine Rosenbæk Gøeg, Zeinab Mahmoudhi, and Anne Sofie Korsager for their company and support. More than anyone, however, I would like to thank my supervisor Johannes Jan Struijk. The contributions which Hans have made to this project are too numerous to be listed here. Instead, here I will only thank Hans for his exceptionally thoughtful and inquisitive ways, which without fail challenges anyone to rethink things more deeply and thoroughly than they had. Most importantly, I would like to thank Hans for his unrelenting and positive focus on future opportunity, which has been instrumental every step of the way.

Ask Schou Jensen

Aalborg University, May 28, 2014

B. English Summary

There is an urgent need for development of new treatments for infectious diseases caused by drug-resistant strains of bacteria such as *mycobacterium tuberculosis* (TB). Increasingly resistant microbial strains are causing disease treatment to become far more difficult, slow, and costly. The discovery of new classes of antimicrobial drugs has halted, and there are few truly novel compounds in the pipeline.

An alternative approach to the development of conventional antibiotics is the development of compounds that reverse antimicrobial resistance. Recent discoveries have demonstrated that the antipsychotic drug thioridazine has both direct antimicrobial activity and the ability to restore sensitivity to conventional antibiotics. This essentially renders them vulnerable to previously ineffective treatments. Thioridazine was used successfully in combination with conventional antibiotics to treat extensively drug-resistant tuberculosis in patients who did not respond to treatment, indicating that thioridazine holds great potential.

There is a problem however. Many compounds within multiple classes of drugs including antipsychotics and antimicrobials have been shown to cause risk of the potentially fatal cardiac arrhythmia Torsades de Pointes. The primary indicator of this risk is QT interval prolongation in the ECG, and thioridazine is indeed QT prolonging. Due to concern over cardiotoxic side effects, branded versions for antipsychotic treatment were withdrawn from the market, and QT prolongation now presents a major obstacle to the introduction of thioridazine for antimicrobial treatment.

The purpose of the work presented in thesis was to investigate a possible solution to this problem. Thioridazine is a chiral compound consisting of a racemic mixture of two similar but chemically distinct molecules: (-)-thioridazine and (+)-thioridazine. Recent findings show that (-)-thioridazine has a substantially reduced antipsychotic effect, whereas their antimicrobial effects are similar. In many drugs an antipsychotic effect is associated with blockade of the cardiac I_{Kr} current, which is the primary cause of Torsades de Pointes. This raises the question of whether (-)-thioridazine also has a reduced cardiotoxic effect.

The primary determinant of QT duration is the ventricular action potential duration (APD). In order to investigate differences in cardiotoxic effects, an experimental setup was established to test the effects of (-)-thioridazine, (+)-thioridazine, and racemate on the APD of the isolated rabbit papillary muscle. The results of this study indicate that both (+)-thioridazine and racemate cause significantly greater prolongation of the APD than does (-)-thioridazine.

Further analysis of experimentally measured drug effects were carried out using computational modeling of the rabbit ventricular action potential. The results of this investigation indicate that the differential effect on the I_{Kr} current can explain the difference in APD prolonging effect.

These results provide the first evidence that isolated (-)-thioridazine may have reduced cardiotoxic side effects. Consequently, (-)-thioridazine may be a safer effective treatment for multidrug-resistant microbial diseases including tuberculosis.

C. Danish Summary

Der er et overhængende behov for udvikling af nye antimikrobielle behandlinger af infektionssygdomme forårsaget af resistente bakteriestammer, inklusive *mycobacterium tuberculosis* (TB). Fordi der er en tiltagende udvikling af resistens mod tilgængelige antibiotika, bliver behandlingen af bakterielle infektionssygdomme stadigt mere udfordrende, tidskrævende og omkostningsrig. Trods dette er opdagelsen af nye klasser af antimikrobielle stoffer reelt standset, og kun meget få reelt nye klasser af stoffer er på vej.

Et alternativ til udviklingen af konventionelle antimikrobielle stoffer er udvikling af stoffer der modvirker antimikrobiel resistens. Nye opdagelser har vist, at det antipsykotiske stof thioridazin har både direkte antimikrobiel effekt og evnen til at omvende bakteriel resistens og derved gøre allerede resistente bakterier sårbare mod tidligere ineffektive antibiotika. Thioridazin er nu også blevet brugt i kombination med konventionelle antibiotika til med succes at behandle patienter med ekstensivt resistent tuberkulose, som ikke responderede på normal behandling. Disse resultater indikerer at Thioridazine har et stort potentiale som et antimikrobielt stof.

Der er dog et væsenligt problem. Mange stoffer indenfor flere klasser af medikamenter inklusive antipsykotika og antimikrobielle stoffer har vist sig at forårsage risiko for tilfælde af den potentielt dødbringende hjertearrytmi *Torsades de Pointes*. Den primære kliniske indikator for denne risiko er forlængelse af QT intervallet i EKGet, og det er påvist at thioridazin er et QT forlængende stof. På grund af bekymring over disse kardiotoksiske bivirkninger blev brandede versioner af thioridazin trukket tilbage fra markedet. Derfor udgør kardiotoksiske bivirkninger en forhindring for introduktionen af thioridazin i antimikrobiel behandling.

Formålet med arbejdet præsenteret I denne afhandling var at undersøge en mulig løsning på dette problem. Thioridazin består af en racemisk 50-50 blanding af to lignende, men stadigt kemisk forskellige molekyler: (-)-thioridazine og (+)-thioridazine. Nye resultater viser, at (-)-thioridazine har væsentligt mindre antipsykotisk effekt, en effekt som ofte er relateret til blokade af den kardielle I_{Kr} ionstrøm, hvilket er den primære årsag til risiko for Torsades de Pointes. Til gengæld ser (-)-thioridazine ud til at have mindst lige så effektive antimikrobielle virkninger som (+)-thioridazine. Disse observationer gør det naturligt at fremsætte hypotesen, at (-)-thioridazine også har reducerede kardiotoksiske bivirkninger.

Det der primært afgør varigheden af QT intervallet er varigheden af det ventrikulære aktionspotentiale (APD). For at undersøge forskelle i kardiotoksisk virkning blev en forsøgsopstilling etableret for at teste virkningen af (-)-thioridazine, (+)-thioridazine og racematen på APD i isolerede papillær muskler fra kaniner. Resultaterne af dette studie indikerer, at både (+)-thioridazine og racematen forårsager større APD forlængelse end (-)-thioridazine. Yderligere analyse af målte aktionspotentialer blev udført ved matematisk modellering af kaninens ventrikulære aktionspotentiale. Resultaterne af dette arbejde indikerer, at blokade af I_{Kr} strømmen kan forklare forskellen i APD forlængende effekt. Disse resultater udgør de første beviser for, at isoleret (-)-thioridazine kan have reducerede kardiotoksiske bivirkninger. Dermed er (-)-thioridazine potentielt en mere sikker effektiv behandling mod multiresistente mikrobielle sygdomme inklusive tuberkulose.

D. List of Papers

I. Ask Schou Jensen, Cristian Pablo Pennisi, Cristian Sevcencu, Jørn Bolstad Christensen, Jette Elisabeth Kristiansen, Johannes Jan Struijk.

Differential Effects of Thioridazine Enantiomers on Action Potential Duration in Rabbit Papillary Muscle

II. Ask Schou Jensen, Cristian Pablo Pennisi, Cristian Sevcencu, Jørn Bolstad Christensen, Jette Elisabeth Kristiansen, Johannes Jan Struijk.

Model Based Analysis of the Effects of Thioridazine Enantiomers on the Rabbit Papillary Action Potential: Part 1

III. Ask Schou Jensen, Cristian Pablo Pennisi, Cristian Sevcencu, Jørn Bolstad Christensen, Jette Elisabeth Kristiansen, Johannes Jan Struijk.

Model Based Analysis of the Effects of Thioridazine Enantiomers on the Rabbit Papillary Action Potential: Part 2

Paper I investigates differential effects of the thioridazine enantiomers on the APD of the isolated rabbit papillary muscle.

Paper II describes the adaptation of an existing computational model of the rabbit ventricular action potential to baseline recordings with the aim of creating a tool for analysis of drug effects.

Paper III analyzes the physiological mechanisms underlying the effects of the thioridazine enantiomers using the adapted model of the rabbit ventricular action potential.

E. Abbreviations

- TB: *mycobacterium tuberculosis*
- MDR-TB: multidrug-resistant TB
- XDR-TB: extensively drug-resistant TB
- TdP: Torsades de Pointes
- ECG: electrocardiogram
- QT interval: time between Q wave onset and T wave end in the ECG
- APD: action potential duration
- SR: sarcoplasmic reticulum
- sub-SL: nonjunctional subsarcolemmal compartment
- CICR: calcium induced calcium release
- I_{Kr}: rapid component of the delayed rectifier potassium current
- I_{Ks}: slow component of the delayed rectifier potassium current
- HH: Hodgkin-Huxley
- I_{Na}: fast sodium current
- I_{K1}: inward rectifier potassium current
- I_{CaL}: L type calcium current
- I_{to}: transient outward potassium current
- I_{tof}: fast component of the transient outward potassium current
- I_{tos}: slow component of the transient outward potassium current
- I_{NaCa}: sodium-calcium exchange current
- I_{NaK}: sodium-potassium pump current
- J_{SRrel}: SR calcium release flux
- J_{SRleak}: SR calcium leak flux
- J_{SRpump}: SR calcium pump flux
- I_{NaBk}: background sodium leak current
- $I_{Cl(Ca)}$: calcium dependent chloride current
- I_{ClBk}: background chloride current
- I_{Kp}: plateau potassium current
- I_{CaP}: sarcolemmal calcium pump current
- I_{CaBk}: background calcium current

Introduction

Background

This thesis addresses the thioridazine-induced prolongation of the cardiac action potential. Thioridazine, a member of the phenothiazine family of compounds, was previously used extensively for its antipsychotic effects. Due to concern over cardiotoxic side effects, thioridazine was eventually withdrawn, as evidence mounted that it causes substantial QT prolongation in the human ECG related to risk of potentially fatal cardiac arrhythmia. However, extensive evidence now also shows that thioridazine has potent antimicrobial activity which makes it effective against multidrug-resistant microbes. This may be very important, as the problems caused by resistance towards available antimicrobial drugs are becoming increasingly severe. Calls have been made for global trials of thioridazine in antimicrobial treatment, but the known cardiac side effects present a substantial barrier towards acceptance of thioridazine for new applications.

The Clinical Problem

There is an urgent need for development of new treatments for infectious diseases caused by drug-resistant strains of bacteria such as *mycobacterium tuberculosis* (TB). Over the past two decades, increasingly resistant strains of TB have appeared - first multidrug-resistant tuberculosis (MDR-TB), then extensively drug-resistant TB (XDR-TB), and now even TB resistant to all antibiotic drugs (1). The WHO estimates that in 2011 there were 310.000 new cases of pulmonary MDR-TB and that 9 % of these cases were XDR-TB (2). This is a serious problem, as treatment in cases of drug-resistant TB is far more difficult and likely to fail due to a lack of effective drugs (3). In addition, development of new antibiotics has dramatically slowed, and most drug development focuses on improvement of already existing classes of antibiotics. There have been no (as yet) successful discoveries of new classes of antibiotics since 1987, and few truly novel agents are in the pipeline (4).

Thioridazine Reverses Antimicrobial Resistance

An alternative approach to the development of conventional antibiotics is the development of compounds that reverse antimicrobial resistance (5). A group of compounds of great interest in this regard is the phenothiazine neuroleptics, which have been widely used for their antipsychotic effect. It was first discovered in the late 19th century that methylene blue, the compound from which the phenothiazines were derived, had antimicrobial activity. Soon after the introduction of the antipsychotic phenothiazine chlorpromazine in the 1950s, anecdotal reports began to occur that patients suffering from TB improved in condition or were cured when treated with this drug. However, due to the successful application of antibiotics at the time, focus remained on the antipsychotic properties of these drugs. In addition, the concentrations required for in vitro antimicrobial effect were clinically irrelevant and the side effects of chlorpromazine were known to be very severe. (6) However, a number of developments have renewed interest in antimicrobial application of phenothiazines. First, the appearance of increasingly drug-resistant microbial strains has caused the need for development of new treatments. Second, it was shown that far lower concentrations of chlorpromazine were required to inhibit the

growth of phagocytized TB (7). During infection, the microbe invades and replicates within human macrophages, and many phenothiazines are accumulated greatly within these cells (6). Third, chlorpromazine was eventually replaced with the related antipsychotic compound thioridazine due to the far milder nature of its side effects, and it was shown that thioridazine has antimicrobial activity similar to that of chlorpromazine (8, 9). This led to a significant amount of research focusing on thioridazine.

It was shown that thioridazine has an in vitro killing effect against phagocytized MDR-TB at a concentration of 0.1 mg L^{-1}, which is well within plasma concentrations reached in chronic antipsychotic treatment (up to 0.5 mg L^{-1}) (10). Following this, in vivo studies in mice showed that thioridazine alone is highly effective against infection with drug-susceptible TB (11) as well as against MDR-TB infection when thioridazine is used in combination with the first-line antibiotic isoniazid (12). In effect, thioridazine is capable of reversing antibiotic resistance and restoring the effectiveness of a previously ineffective antibiotic.

Based on these and similar findings, thioridazine was used to treat a number of XDR-TB patients on a compassionate basis and was shown to improve symptoms and clinical outcomes (6). Most notably, 12 XDR-TB patients not responding to antibiotic treatment were treated with thioridazine in addition to the antibiotics, and this resulted in 11 of the 12 patients being cured (13, 14). These findings indicate that synergistic use of thioridazine with conventional antibiotics is indeed an effective treatment for infection of MDR-TB, XDR-TB, and possibly even totally resistant TB in humans.

It has been argued that the ability of thioridazine to cure XDR-TB is due to three different mechanisms (6): first, thioridazine causes non-killing macrophages to kill phagocytized TB regardless of resistance by inhibiting potassium and calcium transport. Second, thioridazine inhibits the expression of genes that code for efflux pumps that protect TB from noxious compounds. Third, thioridazine inhibits the activity of already existing efflux pumps. Due to this multiplicity of mechanisms, it has been postulated that resistance to thioridazine may not develop due to the high fitness cost of the required adaptations (6).

The Cardiotoxicity of Thioridazine

However, while the side effects of thioridazine are in general less serious than those of chlorpromazine, the cardiotoxicity of thioridazine must be considered a major concern. Initial reports of thioridazine-related ECG changes and ventricular arrhythmia date back as far as 1963 (15), and in particular, the drug has been associated with occurrences of the potentially fatal ventricular arrhythmia *Torsades de Pointes* (TdP). TdP is a polymorphic ventricular tachycardia which was first described by Dessertenne in 1966 (16). This arrhythmia presents in the ECG as an irregular and continuously changing pattern of QRS complex morphology, which has the appearance of the R waves seemingly twisting around an axis (hence the name, which translates as ‘twisting of the spikes’). An example ECG is shown in Figure 1. While most episodes of TdP spontaneously revert to sinus rhythm, sudden cardiac death may also occur.

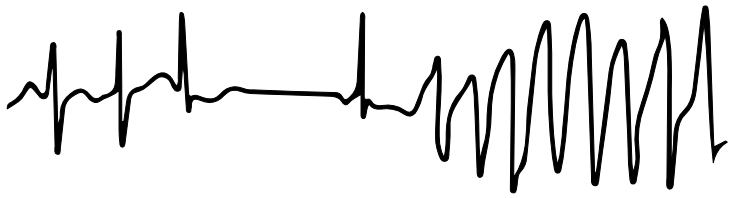

Figure 1: ECG recording during a typical occurrence of TdP. The QT interval is prolonged, and subsequent to an abnormally long RR interval, ventricular arrhythmia occurs.

TdP is thought to be related to heterogeneous ventricular repolarization (17, 18), and occurrences are typically preceded by indications of repolarization abnormality in the ECG. This includes T wave morphology changes, U wave amplitude increase, and QT interval prolongation (19, 20). In particular, prolongation of the QT interval has become a standard surrogate measure of the proarrhythmic risk of pharmacological agents. While controversy exists over the validity of QT prolongation as an indicator of proarrhythmic effect, the importance of this measure in the current context of clinical drug approval can hardly be overstated. The first drug withdrawal due to QT prolongation occurred in 1988, and since then this has become one of the most common causes of withdrawals from the market and denied approvals for new drugs (21, 22). The response of regulators to the problem of repolarization arrhythmia has been establishment of the 'thorough QT study', a clinical phase 1 trial which seeks to identify those drugs that cause QT prolongation beyond a certain threshold. This study is now a requirement for the development of virtually every new pharmacological agent, and failure to pass results in further investigative requirements or even in denied approval. Drugs from a very wide range of important classes of pharmacological agents have been found to be QT prolonging and in some cases to cause risk of TdP, including multiple anti-microbial and anti-psychotic drugs. Studies have now produced overwhelming evidence that thioridazine and two of its primary metabolites, mesoridazine and sulforidazine, cause dose dependent QT prolongation (23-27). It was also found that thioridazine does indeed cause an increased risk of TdP (28-31), and as a consequence of these findings, branded versions of thioridazine were withdrawn in 2005 (32). The QT prolongation of thioridazine consequently also presents a major obstacle towards introduction for antimicrobial treatment.

The Cellular Basis of Cardiotoxicity

The proarrhythmic risk of QT prolonging drugs is associated with blockade of the rapid component of the delayed rectifier potassium current (I_{Kr}), and drugs that have been withdrawn or denied approval due to QT prolongation have consistently had I_{Kr} inhibiting effects (33, 34). It has also been shown that thioridazine indeed does block the I_{Kr} current (35-37). Consequently, it appears highly probable that the proarrhythmic effect of thioridazine is in large part due to I_{Kr} blockade.

The primary determinant of the QT interval duration is the ventricular action potential duration (APD). The I_{Kr} current is a repolarizing potassium current, which in the human ventricular myocardial cell provides an

important contribution to repolarization. Consequently, blockade of the I_{Kr} current prolongs the ventricular APD and this manifests in the ECG as prolongation of the QT interval, see Figure 2. Furthermore, due to heterogeneity in ion channel expression across the ventricular wall, the contribution of I_{Kr} to repolarization is substantially stronger for the midmyocardial M-cells than is the case for the epicardial and endocardial cells. It has been hypothesized, that blockade of I_{Kr} causes an increase in the transmural heterogeneity of repolarization, as M-cells are prolonged to a greater degree than adjacent cellular layers, and that this is a key mechanism in the occurrence of ventricular arrhythmia. This may be particularly exacerbated in case of bradycardial heart rates, as the M-cell APD is prolonged more at lower heart rate, and as APD prolongation due to I_{Kr} blockade tends to be reverse rate dependent, that is to say that greater prolongation occurs at lower rates. Regardless of the mechanisms involved, it is clear that I_{Kr} current blockade plays an important role in the occurrence of TdP. (38-40)

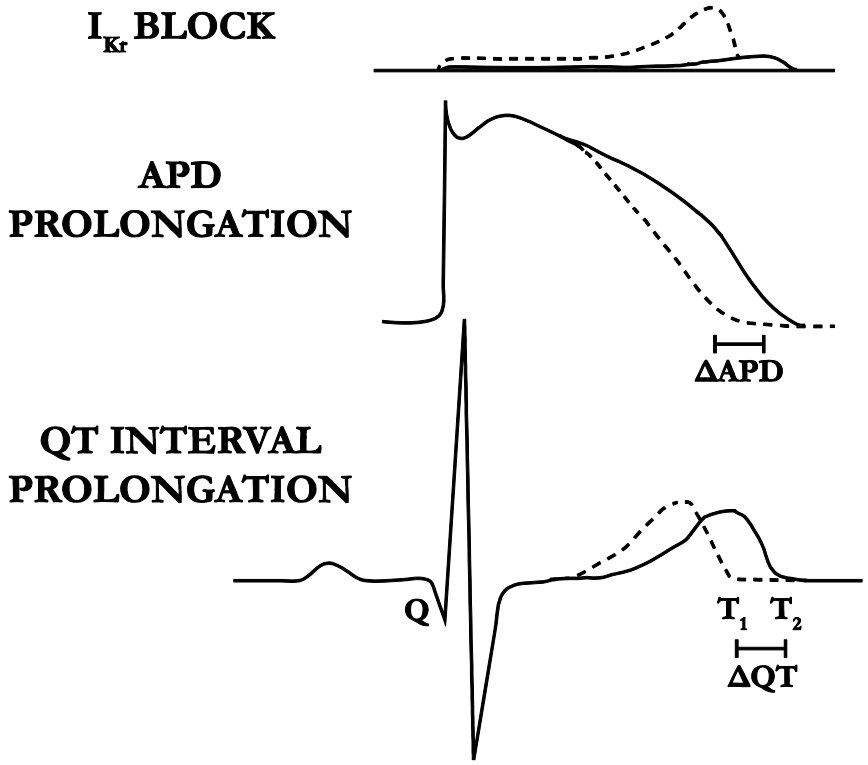

Figure 2: An illustration of the relationship between I_{Kr} blockade, APD prolongation, and QT interval prolongation. The top signal is the repolarizing potassium current through the I_{Kr} channels of the ventricular cell. The middle signal is the action potential, while the bottom signal is the ECG. Dotted lines are baseline signals, while the solid lines show the effect of I_{Kr} blockade. ΔAPD and ΔQT is the resulting APD and QT prolongation. Q indicates the start of the QT interval, while T_1 and T_2 indicate the end of the QT interval before and after IKr blockade.

Stereochemistry – is there a Way Forward?

In addition to the neurological side effects of thioridazine, proarrhythmic I_{Kr} blockade presents a severe problem for the safety profile of thioridazine in antimicrobial applications. However, newer findings regarding the stereochemical properties of the compound suggest that unexplored opportunities may exist.

Stereochemistry has now become an important part of most areas of pharmacotherapy, as many chiral compounds have enantiomers with distinct pharmacological characteristics (41). Thioridazine is such a chiral compound, although it is normally administered as a 50-50 racemic mixture of two enantiomers. These are referred to here as (-)-thioridazine and (+)-thioridazine. The antipsychotic effects of thioridazine are due to blockade of the dopamine D2 receptor, and it has been shown that (+)-thioridazine has 2.7 times the affinity for this receptor in isolated rat brain preparations (42). Greater affinity for the D2-receptor strongly indicates that (+)-thioridazine is the more potent antipsychotic (32, 43). However, the antimicrobial properties of the enantiomers are similar and in some cases stronger for (-)-thioridazine (44-46). In addition, (-)-thioridazine accumulates to a greater extent in human tissue (47).

The apparent difference between thioridazine enantiomers suggests an interesting hypothesis – that the enantiomers may also have different cardiotoxicity. This hypothesis is supported by the fact that many D2 dopamine receptor blocking antipsychotics also prolong the QT interval and in some cases cause a risk of TdP (48, 49). If the lower affinity of (-)-thioridazine for the D2 receptor is associated with a lower affinity for blockade of the I_{Kr} current, then it is quite possible that (-)-thioridazine has both less severe neuroleptic and cardiotoxic side effects than (+)-thioridazine while having similar antimicrobial activity. In this case, the isolated (-)-enantiomer may be a safer treatment than the racemate, and an important obstacle to introducing thioridazine for antimicrobial treatment will have been overcome.

Investigating Thioridazine Enantiomer Effects

It is clear that there is a need for investigation of the effects of the isolated thioridazine enantiomers on ventricular repolarization. Ultimately, an absolute requirement will be a determination of the effect of the isolated enantiomers on the QT interval in humans. With the aim of advancing towards this goal, studies first need to be carried out in an experimental animal model. Such studies may be carried out on several levels, including that of the ECG arising from the electric activity of the *in situ* heart, the level of the action potential of the single cell in isolated heart preparations, and on the level of the individual ion channel current. While full determination of differences in effect should ideally involve investigation on all these levels, an initial investigation should aim to verify whether there indeed is a difference in the effect of the enantiomers on the duration of repolarization. Investigating this through measurement of the individual action potential is a useful initial approach, as this provides direct indication of the activity of the drug at a relatively detailed level and under highly controlled conditions. There are a range of animal experimental isolated heart preparations available in which the effects of compounds may be investigated. The choice of preparation is important and must be made with the goals of the study in mind.

A central aspect that must be considered is the choice of an animal model. The physiology of ventricular repolarization in the selected animal must be relevant to the information desired about potential effects on human repolarization. Due to the central role of I_{Kr} current blockade in the occurrence of TdP, a central aspect must necessarily be to investigate differences in the I_{Kr} inhibiting effects of the enantiomers. The I_{Kr} current does not play a substantial role in ventricular repolarization in the adult rat and mouse which makes these species unsuitable. Larger rodents commonly used in experiments and which may be housed at the available facilities include the guinea pig and rabbit. The slow component of the delayed rectifier potassium current (I_{Ks}) contributes strongly to repolarization in the guinea pig, while the impact of I_{Ks} blockade on the QT segment duration and APD in multicellular ventricular preparations is negligible in the rabbit (50, 51). However, I_{Kr} current blockade does cause measureable APD prolongation in the rabbit (51). This makes the rabbit well suited for investigating the effects of I_{Kr} inhibition. A standard experimental preparation for measuring the rabbit ventricular action potential is the isolated rabbit papillary muscle. This is the experimental preparation which was used for the work presented in this thesis and it is described in detail in the section starting on page 19.

While the difference in APD prolonging effect between the thioridazine enantiomers is of central importance, this measure alone does not directly demonstrate the nature of the exact mechanisms responsible. Over the past few decades, computational modeling of the cardiac electrophysiology has made substantial leaps forward, as increasingly detailed and descriptive models of the ventricular cell have been developed using extensive data from a number of species, including the rabbit (52). A mathematical model may be used to indicate where existing knowledge is incomplete and to make predictions on which to base further empirical investigation. A sufficiently descriptive model of the investigated system may aid in integrating empirical data with existing knowledge in order to further the analysis and understanding of these results. In order to investigate the physiological basis of the effects of the thioridazine enantiomers, an investigation of the drug effects was carried out based on the acquired empirical data and a modified version of an existing computational model of the rabbit ventricular action potential. This model is described in the section starting on page 23.

Objectives of the Thesis

The purpose of the work presented in this thesis was to confirm or reject the hypothesis that the enantiomers of thioridazine have dissimilar effects on the duration of repolarization in the ventricular cell of a representative animal model and to characterize these differences, if present. This was done using transmembrane action potential recordings in a standard preparation - the isolated papillary muscle.

The secondary objective was to explore the physiological basis of the differences using computational modeling of the ventricular papillary muscle cell. In particular, the goal was to test the hypothesis that a difference in prolonging effect between the enantiomers can be explained by a difference in affinity for blockade of the I_{Kr} current.

The Isolated Rabbit Papillary Muscle

Prior to the work presented in this thesis, there was no experimental setup available at our department for investigation of drug effects on the ventricular action potential. For this reason, such a setup was established for use with the isolated papillary muscle preparation. This chapter provides an overview of the properties of this preparation and a description of the experimental setup and primary methods. The focus here is on those aspects which are not covered in detail in the included publications.

The Experimental Preparation

The isolated papillary muscle is a widely used experimental preparation in cardiovascular research, as it is well suited for investigating the effects of pharmaceutical compounds, ionic imbalances, and hypoxia on contraction and cellular electrophysiology (53). The papillary muscles are of course located within the left and right ventricles and are continuous with the endocardium, see Figure 3. They attach via the chordae tendineae to the atrioventricular valves, and contraction of the papillary muscles serves to prevent inversion of the valves during ventricular contraction.

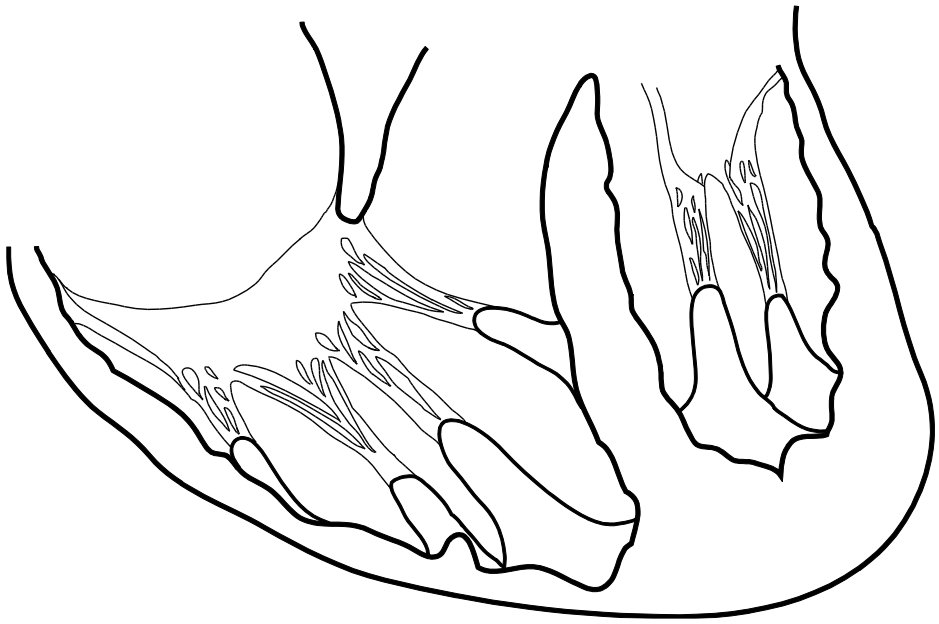

Figure 3: Illustration of the papillary muscles located within the right and left ventricles.

The isolated papillary muscle has a number of properties which makes it particularly well suited to electrophysiological study. While the papillary muscles display considerable anatomical variance, the ventricles contain a number of muscles from which a preparation may be created. Papillary muscles vary in number, size, and shape (a bifurcated shape is relatively common), but the right ventricle almost invariably contains one or more papillary muscles of the thin, elongated, non-bifurcated type. This anatomical type tends to have a base of a small diameter, meaning that the muscle may be excised from the endocardium with minimal damage.

Conversely, the papillary muscles of the left ventricle tend to be relatively short and attach to the endocardium over a much greater area. An elongated shape allows measurements to be made relatively far from the cutting surface and the point of electrical stimulation, minimizing undesired interference with the measurement site. Importantly, the thin diameter of the muscle allows it to be sustained by simple superfusion, as saline solution is able to diffuse through the muscle (53). In a thicker muscle, the core should be expected to become ischemic under superfusion due to restriction of diffusion. This also sets the isolated papillary muscle apart from preparations involving the whole heart or larger sections of the myocardium, which typically require coronary perfusion. The relatively small size of the papillary muscle also means that muscular contraction results in relatively limited displacement at any point on the muscle surface. As a consequence, stable impalement of a single myocardial cell may be maintained in order to directly record the single cell transmembrane potential, whereas the displacement involved in a whole heart preparation necessitates the recording of monophasic action potentials instead. For these reasons, the isolated papillary muscle was used in the studies presented in this thesis.

The Experimental Setup

All procedures involving living animals were carried out by qualified technicians. The animal was sedated and anesthetized, and once the animal was confirmed to be fully sedated, it was killed by a strong blow to the neck. After the animal was confirmed to be dead, the heart was rapidly excised and washed in a cold saline solution in order to remove blood prior to the onset of coagulation. While submerged in cold saline, the right ventricular wall was opened, and papillary muscles of the elongated type were carefully excised and transferred to an organ bath for use in the experiment, see Figure 4. For electrophysiological measurements, the muscle was mounted with fine pins through the base and *chordae tendineae* in a horizontal position. This position allowed a microelectrode to be maneuvered to a suitable location on the muscle surface using a microscope located above the preparation. At all stages, the saline solution was maintained at appropriate temperature and continuously saturated with a gas appropriate to the buffering agent in order to ensure oxygenation and proper pH value. It was not possible to gas directly in the bath, as bubbles cause ripples in the solution. This displaces the microelectrode and may cause instability in the impalement. (53)

The bath was secured on a vibration resistant table, and a peristaltic pump was used to recirculate the solution, achieving a continuous and stable inflow and outflow of saline solution. A chamber used to gas the solution and to introduce new solution was located prior to the bath. Between this chamber and the bath was a spiral contained in a cylinder of heated water. The heating occurring in this spiral maintained the temperature of the solution in the bath, which was also continuously monitored. A diagram of the experimental setup is shown in Figure 5.

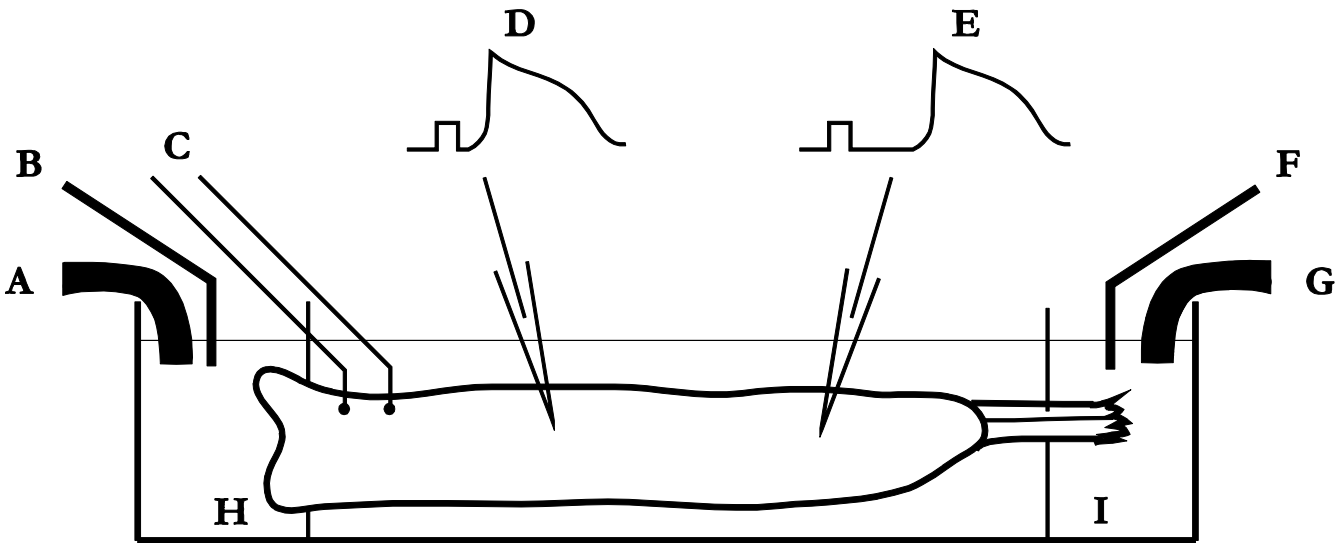

Figure 4: Papillary muscle mounted in organ bath. A: saline inflow. B: temperature probe. C: stimulation electrode. D: action potential recorded near the stimulation site. E: action potential recorded distant from the stimulation site. F: reference electrode. G: saline outflow. H: basal mounting pin. I: chordae tendinae mounting pin. As can be seen, depolarization propagates through the muscle, and greater distance between stimulation site and measurement site results in a longer delay between stimulation artifact and action potential upstroke.

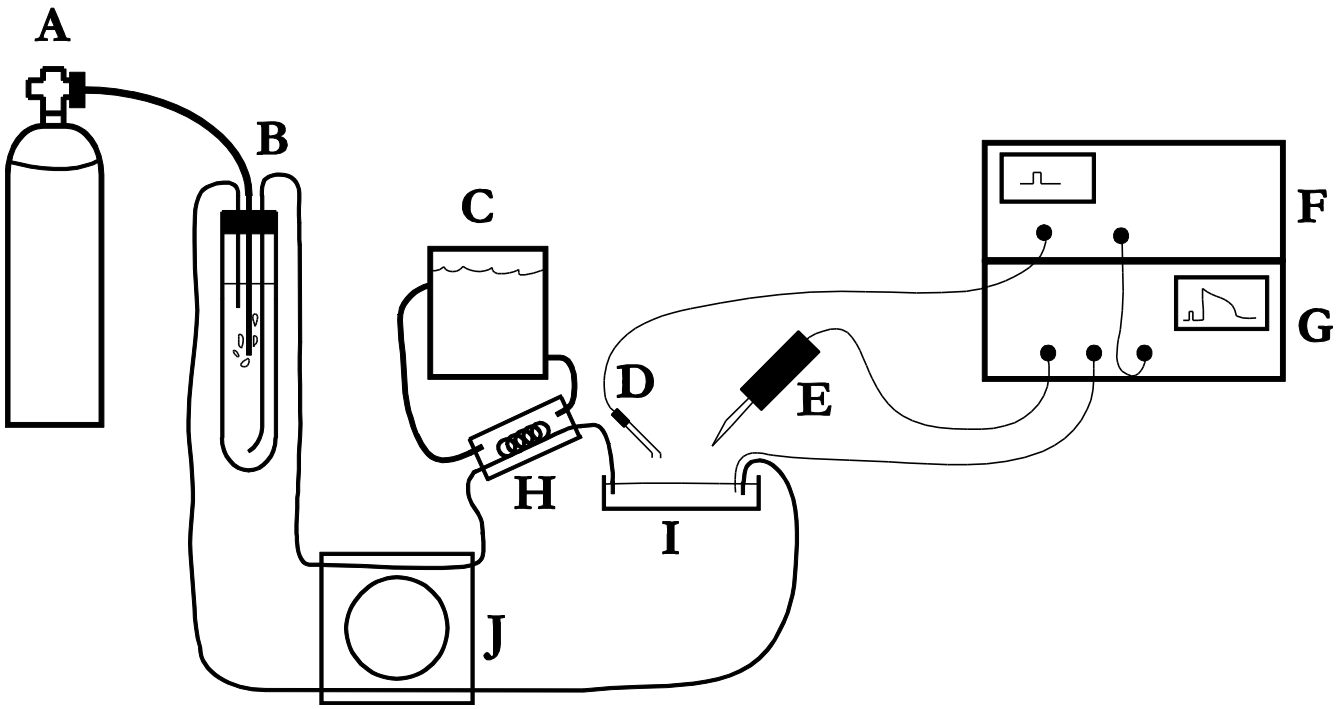

Figure 5: Diagram of the experimental setup. A: carbogen canister. B: gassing cylinder. C: heater. D: stimulation electrode. E: micromanipulator mounted micropipette. F: digital stimulator. G: amplifier. H: heating spiral. I: organ bath. J: peristaltic pump.

The papillary muscle was stimulated at the base with a stimulation electrode, causing a wavefront of depolarization to propagate through the muscle and triggering an action potential at the measurement site. The stimulation threshold was found manually by varying the pulse amplitude and visually confirming muscle contraction. The muscle was continuously stimulated with a square pulse with double the amplitude of the stimulation threshold. Triggered by the stimulator, measurements were carried out using a saline filled, sharp, high-impedance, glass micropipette created by pulling apart a glass filament with a micropipette puller. The microelectrode was filled with a 3M KCL solution and mounted on a hydraulic micromanipulator. The electrical potential was measured with respect to a reference electrode placed in the bath. Using the micromanipulator and a mounted microscope, the tip of the micropipette was carefully maneuvered to the edge of the papillary muscle. The muscle was impaled, and by means of very fine and careful movements, a stable impalement of a single cell was achieved by observation of the resting membrane potential and triggered action potentials. (53) Figure 6 shows an example of a recorded action potential.

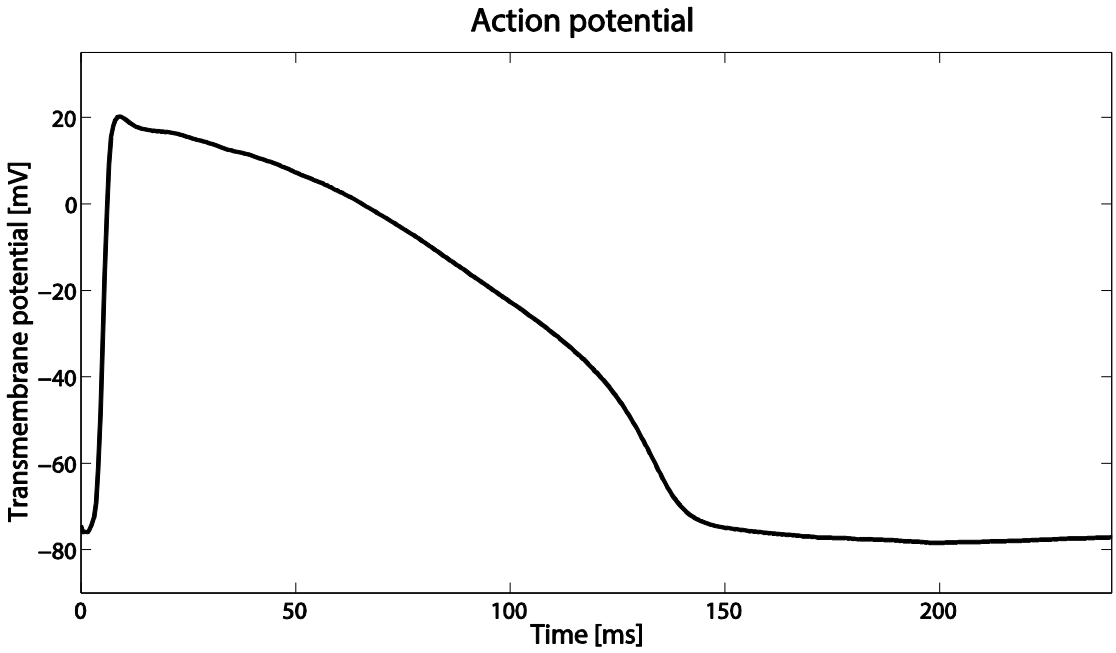

Figure 6: an example of a median action potential recorded at baseline conditions.

Investigation of Drug Effects by Computational Modeling

Modeling of the Action Potential

The action potential and excitation-contraction coupling of the ventricular cell arises due to a complex system consisting of many subsystems, each of which has direct or indirect effects on all other subsystems. Each subsystem may be studied empirically in isolation, but due to interaction between systems, the difficulty of studying the simultaneous functioning of multiple systems becomes great. At a certain level of complexity, a potentially more fruitful approach is to use mathematical modeling to characterize each subsystem with equations that describe laboratory experiments, and then to combine these parts into a more comprehensive model in which interactions may be studied more readily. While a mathematical model of such complex interactions can never be perfect, and while a model is not as useful as direct empirical data, nevertheless, an integrated model may be a powerful tool to improve understanding and guide thought, investigation, and analysis. (52)

A great number of cardiac action potential models are now available, focusing on different species, cell types, cell components, behaviors, and levels of complexity. In addition there has been a long history of development during which models have gradually grown in both complexity and descriptive power as greater understanding of the modeled mechanics were understood and as more data of higher quality became available. Models now take into account many aspects of the cardiac cell including membrane voltage, cellular geometry, membrane channels, pumps, and transporters, ion concentrations in multiple compartments, buffering systems and binding molecules in both cytoplasm and the sarcoplasmic reticulum (SR), and calcium induced calcium release (CICR). (54)

The Hodgkin-Huxley Membrane Current Formulation

There are many similarities between the membrane currents of the myocardial cell and the nerve cell. Despite the ever increasing complexity of new models, modern modeling of the myocardial membrane currents owes much to Hodgkin and Huxley, whose work resulted in the 1952 publication of the now classic Hodgkin-Huxley (HH) model, which describes the action potential of the squid giant axon (55). The formulation of the membrane ion channels in the HH model still represents the basic formulation used in most modern models.

The action potential of course arises due to the net electrical current resulting from ion flux across the cellular membrane. Individual ions move through specialized pore-forming proteins creating channels through the membrane, which may be very specific to an ionic species. Such channels may be gated, responding stochastically to external stimuli by opening for a short time and then rapidly returning to an inactivated state. Due to the large number of channels across the membrane, this stochastic process gives rise to an observable and predictable net ion current. (54)

The driving force for movement of charged particles across a passive channel is the result of the electrochemical gradient across the membrane. Passive net movement of charged particles against the

concentration gradient occurs only if the driving voltage difference is sufficiently great. Thus, the most basic formulation of an ion current across a membrane with conductance selective for that ion is given by Eq. 1. (54)

$$I = \bar{g}(V_M - E) \quad \text{Eq. 1}$$

Here, $\bar{g}$ is the maximal current conductance, V_M, is the membrane voltage, and E is the (Nernst) reversal potential for the specific ion.

The maximal conductance of an ion current may be described by Eq. 2.

$$\bar{g} = N\bar{g}_1 \quad \text{Eq. 2}$$

Here, N is the number of channels and $\bar{g}_1$is the unitary conductance - the conductance of a single channel.

As seen in Eq. 1, the driving force for an ionic species is the difference between the membrane voltage and the reversal potential for that ion. The reversal potential is the potential difference across the membrane at which no net flux of the ion occurs as the chemical and electrical gradients exactly balance each other out. From the Nernst equation, the reversal potential is given by Eq. 3. (54)

$$E = \frac{RT}{zF} ln \frac{Y_o}{Y_i} \quad \text{Eq. 3}$$

Here, R is the universal gas constant, T is the absolute temperature, F is the Faraday constant, z is the valence of the ion in question, and $ln\frac{Y_o}{Y_i}$ is the natural logarithm of the ratio between extracellular and intracellular ion concentrations. The greater this ratio, the greater is the membrane voltage required to overcome the concentration gradient.

Voltage sensitive gating changes the state of the channel to allow or disallow movement of ions. Each gate is represented by a normalized variable with value between 0 and 1, representing the fraction of channels that may be found in the open state. For example, in the HH model the Na^+ channel current is modeled by three voltage dependent activation gates and one voltage dependent inactivation gate, see Eq. 4. (54)

$$I_{Na} = \bar{g}_{Na} m^3 n (V_M - E_{Na}) \quad \text{Eq. 4}$$

Here, m is an activation gate and n is an inactivation gate. The activation gate opens in response to depolarization, allowing rapid depolarizing influx of Na^+, which triggers the action potential. The inactivation gate closes in response to depolarization, halting Na^+ influx.

Gating variables are described by their own differential equations. For example the change in state of the m activation gate is defined by Eq. 5. (54)

$$\frac{dm}{dt} = \alpha_m(1 - m) - \beta_m m = \frac{m_\infty(V) - m}{\tau_m(V)} \quad \text{Eq. 5}$$

Here α_m is the rate of opening, $\beta_m$is the rate of closing, m_∞ is the steady state fraction of gates in the open state given a voltage level, and τ_m is the time constant of state transition. Thus, the change in fraction of gates in the open state depends on the rate of opening and closing and the fraction of gates already in the open state. Ultimately, the behavior of the voltage sensing gate is determined by these transition rates, which are voltage dependent variables. Increasing voltage causes the rate of transition to both the open and inactivated state to increase, leading to a rapid net opening of channels and subsequent inactivation. The drop in membrane potential following from repolarization causes a transition away from inactive state to a resting nonconducting state, from which reopening can occur. The voltage dependence of transition rates typically follows sigmoidal curves. Due to the voltage regulation of transition rates, the voltage determines both the steady state fraction of m gates in the open state m_∞ and the time constant τ_m with which m tracks m_∞.

Alternative Membrane Channel Formulations

The HH channel formulation describes the case of a membrane channel which is selective for a single ionic species. However, such selectivity may not be ideal, and some currents may carry multiple ionic species with different conductivities. The Goldman-Hodgkin-Katz equation (or Goldman equation) is a generalization of the Nernst equation which is used to derive the potential across a membrane with conductivity to multiple ionic species with different chemical gradients. This equation is often used to model currents that are not assumed to be ideally selective.

An important alternative to the HH formulation of channel gating is the Markov chain model. In this formulation, channels may inhabit one of a number of states, with stochastic transitions happening between states of the channel. For example, in a simple model the channel may inhabit an open, closed, or inactivated state, and the behavior of the current would be determined by six rates of transition among these three states. Markov chain models may model certain aspects of channel behavior such as dependence between channel activation and inactivation more accurately than the HH formulation. However, the complexity and computational demands are also greater. (54)

From Hodgkin and Huxley to the rabbit ventricular cell model

While the HH model provides the basic formulation of ionic currents used in most models, there have been many advances involved in the development of cardiac cell modeling. These form the basis of the of the rabbit ventricular cell model used in this study. A brief overview of several important advances leading to the development of this model will be presented here.

Following the discoveries of Hodgkin and Huxley, extension of this work to describe cardiac cell types happened very slowly due to experimental challenges and the greater complexity of the cardiac action potential (56). The first model of a cardiac cell, the 1962 Purkinje cell model published by Noble (57), predates the discovery of Ca^{2+} current in cardiac cells. Only by the mid-1970s was data sufficient for the development of more descriptive cardiac models available, and in 1975 McAllister et al. published a model of the Purkinje fiber including both inward Ca^{2+} current and multiple potassium currents (56), which had now been discovered. In 1977, the first model of the ventricular myocardial cell was published by Beeler and Reuter. This was a generic mammalian model incorporating four ion currents including fast inward sodium (I_{Na}), a time-dependent outward potassium current (which would later become I_{Ks} and I_{Kr}), a time-independent outward potassium current (I_{K1}), and a slow inward Ca^{2+} current (which would later become the L type Ca^{2+} current, I_{CaL}) (58).

These models were still limited by inadequate experimental techniques and a lack of data on ion concentrations in the extracellular cleft. With the development of patch clamp techniques in the late 1970s and early 1980s, single channel recordings became possible, overcoming previous experimental barriers by allowing direct quantitative description of channel kinetics. In addition, it became possible to control intra- and extracellular ion concentrations. (59) These important advances led to the development of the 1985 model by DiFrancesco and Noble of the cardiac Purkinje cell. This model was the first to track K^+ and Na^+ concentrations and to include advanced Ca^{2+} dynamics including Ca^{2+} sequestration in the SR and also CICR. In addition, the model was the first to include the Na^+-K^+ pump, an ATP driven mechanism maintaining ionic gradients by extruding Na^+ in return for K^+, and also the first to include the Na^+-$Ca2^+$ exchanger, a concentration gradient driven mechanism which extrudes Ca^{2+} in return for Na^+. (60)

In 1991, Luo and Rudy published the first version of what would in practice become the standard ventricular cell model (59). This model of the guinea pig ventricular myocyte was the first ventricular model to describe a specific species rather than a generic mammalian cell. It was based on the model of Beeler and Reuter and updated the currents of this model with recently acquired data. It also added several currents including plateau and background K^+ currents. The second version was published in 1994 (61). This version included many of the elements also introduced by DiFranceso and Noble but used new data primarily from the guinea pig ventricular cell. The I_{CaL} current was reformulated from the slow inward current of the Beeler and Reuter model to include faster activation and also voltage- and calcium-dependent inactivation. The Na^+-K^+ pump and Na^+-Ca^{2+} exchanger were included as was a nonspecific Ca^{2+}-activated current and a Ca^{2+} pump. In addition, the SR was introduced which was divided into two functional and anatomical compartments, the junctional and the network SR, comprising 8% and 92% of the total SR volume respectively. An uptake current moved Ca^{2+} ions from the cytoplasm to the network SR, from where they would translocate to the junctional SR. CICR occurred from the junctional SR to the cytoplasm, and a leakage current was present from the network SR to cytoplasm

also. The model tracked intracellular K^+, Na^+, and Ca^{2+} concentrations and the Ca^{2+} concentration in the SR as well. Buffering of Ca^{2+} was accounted for in both the cytoplasm and SR. Further updates were introduced through the 1990s and 2000s. In 1995, Zeng et al. divided the time-dependent outward potassium current into the I_{Kr} and I_{Ks} currents and updated the Ca^{2+} buffering (62). In 1999, Viswanathan et al. reformulated I_{Ks} and CICR and introduced heterogeneous I_{Kr} and I_{Ks} expression to differentiate endocardial-, epicardial-, and midmyocardial cells (M-cells) (63). In 1999, Clancy and Rudy included a Markov chain model of I_{Na} to simulate the effect of genetic mutations (such as in long QT-3 syndrome and Brugada) (64), and in 2000, Faber and Rudy introduced Na^+ activated K^+ current and modified the sarcoplasmic Ca^{2+} release and Na^+-Ca^{2+} exchange (65).

In the late 1990s, the Winslow group developed a model of the canine ventricular cell based on the Luo-Rudy model modified using canine data (66, 67). This model represented a major step forward in the modeling of ventricular Ca^{2+} homeostasis, as several new discoveries were incorporated (52). This included new formulations of the Ca^{2+} inactivation of the I_{CaL} current and Ca^{2+} regulation of the ryanodine receptor – the sarcoplasmic channel responsible for CICR. Importantly, this model also included a junctional subspace, an anatomical volume of the intracellular space between the junctional SR and the T tubule membrane. This subspace was where the CICR occurred, as I_{CaL} channels and the ryanodine receptors were localized here. Consequently, the Ca^{2+} concentration could increase locally to much greater levels than in the bulk cytoplasm. The model also included troponin binding sites for Ca^{2+}. (66, 67)

The first model of the rabbit ventricular cell was published by Puglisi and Bers in 2001. This model was based on the Luo-Rudy model but with many currents rescaled to match data from the rabbit ventricle. The model included the transient inward potassium (I_{to}) current, which is present in the rabbit but not in the guinea pig. It also included a Ca^{2+} activated Cl^- current and made modifications to the kinetics of I_{Kr} and T type Ca^{2+} current. (68)

In 2004, Shannon et al. of the same group published a new Rabbit ventricular cell model. This was based on the model of Puglisi and Bers and included the advances in Ca^{2+} modeling introduced by the Winslow group. Consequently, the Shannon model was of course directly based on the Luo-Rudy model, as this formed the basis of both previous models. The Shannon model was based on new data acquired from the rabbit ventricle, and it also included several novel features. A subsarcolemmal compartment was introduced which allowed membrane channels to sense ion concentrations different from those in the bulk cytoplasm. This model also introduced a reversible Ca^{2+} pump in the SR and new formulations of the Na^+-Ca^{2+} exchanger and the ryanodine receptor. (52)

The Shannon Model of the Rabbit Ventricular Cell

Paper 2 and 3 presented in this thesis were based on the 2004 Shannon model of the ventricular rabbit cell. This section will present an overview of the structure and components of this model.

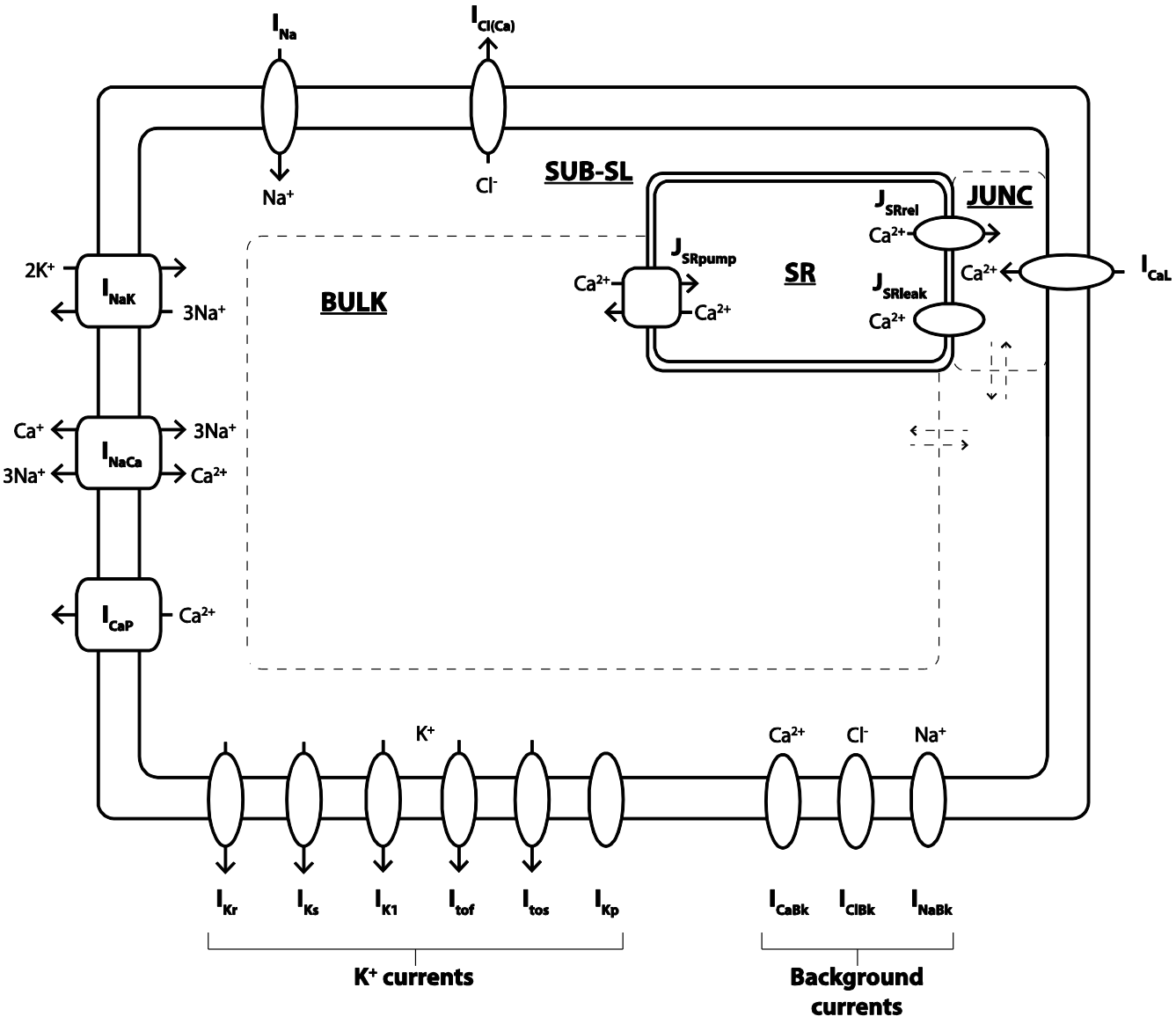

Figure 7: a diagram showing the structure and components of the Shannon rabbit ventricular cell model. Dashed lines separate compartments which are not physically divided by membranes and between which passive diffusion occurs, which is indicated by dashed arrows. Double solid lines indicated separation of compartments by membranes. Ovals indicate ion channels while squares indicate pumps and transporters. SR: sarcoplasmic reticulum. Bulk: bulk cytoplasm. Sub-SL: subsarcolemmal subspace. Junc: junctional subspace. Currents are described in the text.

The Shannon model simulates the rabbit ventricular cell at a temperature of 37°C. The model consists of four compartments, see Figure 7. These include a bulk cytoplasmic space (65% of total cell volume), the SR (3.5%), a junctional cleft (0.077%), and a nonjunctional subsarcolemmal (sub-SL) compartment (2%). The remainder of the nonmyofibrillar cell volume is assumed to be taken up by mitochondria, which do not play a role in the

model. The sub-SL compartment is a narrow space just under the remainder of the sarcolemma where diffusion is restricted due to the presence of mitochondria and myofilaments. The sub-SL is not an anatomical compartment, but a functional one, where Ca^{2+} concentrations can exceed those of bulk cytoplasm due to restricted diffusion. The presence of such a gradient in Ca^{2+} concentration is indicated by experiments, and this explains why certain membrane channels are regulated by Ca^{2+} concentrations higher than those found in the bulk. Unlike previous models, the SR consists of only a single compartment. The junctional cleft is similar to the junctional space introduced by the Wilson group. Diffusion between the junction and sub-SL is restricted due to the narrow boundaries of the junction and the presence of large proteins. (52)

Ions diffuse between the junctional cleft and the sub-SL space and between the sub-SL space and bulk cytoplasm. The model tracks intracellular Na^+ and Ca^{2+} concentrations in all cytoplasmic compartments and Ca^{2+} in the SR. Extracellular ion concentrations and the intracellular K^+ concentration is assumed to be constant. Buffering of Na^+ is assumed to be significant only near the sarcolemma and Na^+ buffers are thus only present in the junctional cleft and sub-SL compartments. The model contains a number of Ca^{2+} buffers and binding molecules distributed over all compartments. (52)

The SR contains ryanodine receptors giving rise to Ca^{2+} release flux (J_{SRrel}), a passive Ca^{2+} leak flux (J_{SRleak}), and the ATP driven SR Ca^{2+} pump (J_{SRpump}). Ryanodine receptors are entirely located in the junctional cleft, and all Ca^{2+} release occurs into this compartment. The receptor is modeled with a Markov chain of four possible states: closed, open, inactivated, and resting inactivated. Ca^{2+}influx in the junctional cleft causes Ca^{2+} to bind to both fast activation sites and slow inactivation sites, causing channels to transition to the open and then inactivated states. Ca^{2+} concentration decline causes a transition to the resting inactivated and finally closed states. The ryanodine receptor is affected by Ca^{2+} binding sites inside the SR. Higher Ca^{2+} load augments transition to the open state, resulting in greater Ca^{2+} release. Like the ryanodine receptor, passive leak flux also occurs between the SR and junctional cleft. ATP driven Ca^{2+} uptake on the other hand, occurs entirely from the bulk cytoplasm. The pump uses a novel formulation that includes reversibility as seen in experiments, although the net flux is always in the same direction. (52)

Membrane channels are evenly distributed between the sub-SL and junctional areas of the sarcolemma. Due to the difference in membrane surface, these channels are distributed with 89% in sub-SL compartment and 11% in the junctional cleft. For I_{CaL} however, 90% of channels are concentrated in the junctional cleft, where CICR occurs. The major membrane currents at 2 Hz steady state pacing are shown in Figure 8 and Figure 9. (52)

Na^+ currents include the fast Na^+ current (I_{Na}) and a background Na^+ leak (I_{NaBk}). Both used the same equations as in the Luo Rudy model. The model also includes two Cl^- currents, a Ca^{2+} dependent Cl^- current ($I_{Cl(Ca)}$), and a passive background Cl^- current (I_{ClBk}). (52)

K^+ currents include the I_{Kr}, I_{Ks}, I_{to}, and I_{K1} currents and also a passive plateau K^+ current (I_{Kp}). All K^+ currents except I_{Ks} were modified versions of the formulations in the Luo Rudy model. I_{Kr} uses a Hodgkin-Huxley formulation with a single activation and inactivation gate, and a maximal conductance dependent on extracellular K^+. I_{Ks} has two voltage dependent activation gates, the maximal conductance is regulated by intracellular Ca^{2+}, and the equilibrium potential for I_{Ks} also depends on the Na^+ gradient across the membrane.

The I_{to} current is divided into two separate components: fast and slow I_{to} (I_{tof} and I_{tos}), both including voltage regulated activation and inactivation gates. I_{K1} is a voltage gated inwardly rectifying current, and similarly to I_{Kr}, the maximal conductance is dependent on extracellular K^+ concentration. (52)

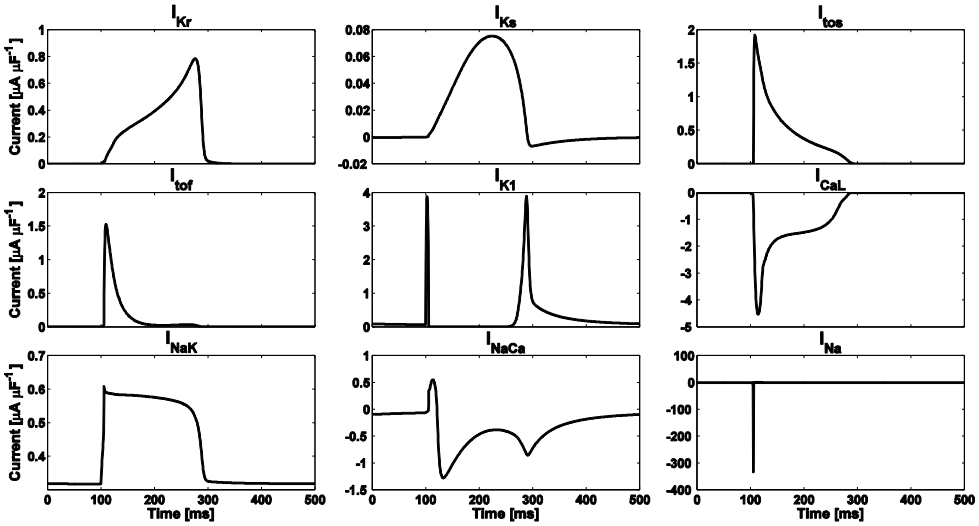

Figure 8: the major transmembrane currents of the rabbit papillary model as represented in the Shannon rabbit cell model in 2Hz steady state pacing. Negative current is depolarizing. Each plot uses a different ordinate axis.

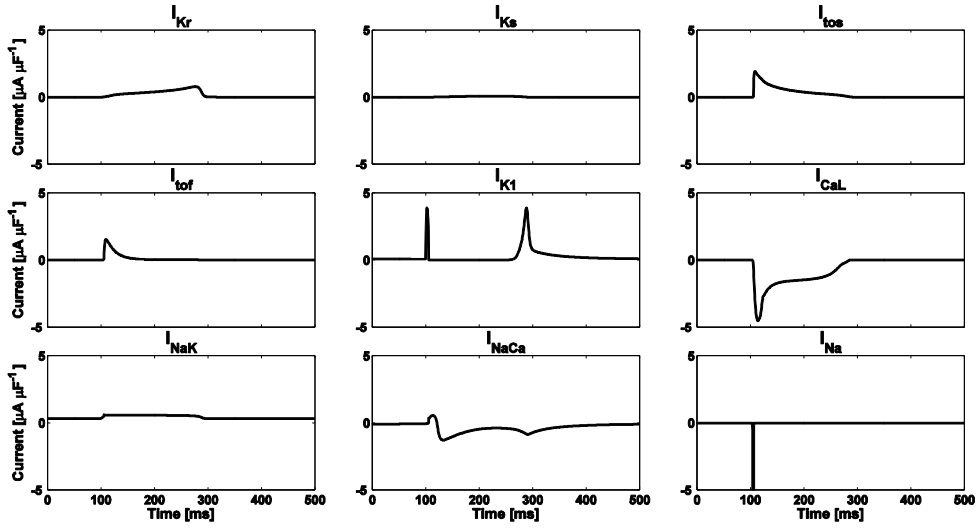

Figure 9: the major transmembrane currents of the rabbit papillary model as represented in the Shannon rabbit cell model in 2Hz steady state pacing. Negative current is depolarizing. All plots are scaled to have identical ordinal axes.

Ca^{2+} currents include the I_{CaL} current, an ATP driven sarcolemmal Ca^{2+} pump regulated by the Ca^{2+} concentration near the membrane (I_{CaP}), and a passive background Ca^{2+} leak current (I_{CaBk}). The model does not include a T type Ca^{2+} current, as this is not detectable in normal rabbit myocytes. The I_{CaL} current is a modification of the formulation in the Luo-Rudy model based on the Goldman-Hodgkin-Katz equation. However, the permeabilities to Na^+ and K^+ were decreased to match experimental data when all three ions are present. The channel is voltage activated and includes both fast and slow voltage regulated inactivation and Ca^{2+} inactivation. The Ca^{2+} inactivation was modified to depend on the Ca^{2+} binding messenger protein Calmodulin. (52)

The model also includes the Na^+- K^+ pump (I_{NaK}) and the Na^+-Ca^{2+} exchanger (I_{NaCa}). I_{NaK} uses the formulation of the Luo Rudy model and extrudes Na^+ in return for K^+ in a 3:2 ratio. I_{NaCa} is a reversible transporter which uses the concentration gradient to exchange Na^+ for Ca^{2+} in a 3:1 ratio. In the forward mode it removes Ca^{2+} from the cell, which is the primary mode of action, but following Na^+ influx it may temporarily operate in the reverse mode. Despite the forward mode functioning to extrude Ca^{2+}, the current is primarily depolarizing due to the reverse Na^+ influx. The I_{NaCa} current in the Shannon model uses a novel formulation. It is activated by binding of Ca^{2+} to a site on the inside of the membrane and is deactivated as the Ca^{2+} transient falls after release and Ca^{2+} disassociates from the binding site. This causes the exchanger to turn off near the resting level of the intracellular Ca^{2+} concentration. Unlike the formulation in the Luo Rudy model, it also accounts for regulation due to intracellular Na^+. (52)

Modifications

The Shannon model was developed using data from a wide variety of sources under different conditions. In order to more realistically characterize the effects of drugs for the specific preparation used under the specific circumstances of this experiment, there was a need to adapt the model to better describe action potentials under baseline conditions. Thus, in the work presented in this thesis, the ion channel currents in the Shannon model were adapted to model both baseline action potentials and drug effects. Adaptations were carried out by change in maximal current conductances, which is the product of the number of channels and the unitary conductance, see Eq. 2. Thus, these adaptations had no direct impact on channel kinetics. Instead, in the case of adaptation to baseline recordings, this modeled the density of channels present in ventricular cell. In the case of drug effects, these were consequently modeled as effects on the density of channels able to pass current and/or effects on the unitary conductance of those channels.

The model action potential depends strongly on multiple factors including pacing rate and inhibition of membrane currents. A change in these factors induces a change in the steady state, which the modeled action potential model may require several minutes of simulated time to reach. This greatly increases the computational cost of investigating the effect of varying parameter values. In order to overcome this barrier, an additional adaptation was carried out. This did not alter the functioning of the model but only caused the initial state to be dependent on parameter values, and it enabled an identical steady state to be reached much faster. It was identified that changes in APD due to changes in pacing rate were almost entirely subsequent to

relatively fast changes in sarcoplasmic Ca^{2+} load (changes over seconds) and very slow changes in bulk cytosolic Na^{+} concentration (changes over minutes). In paper III, the I_{CaL}, I_{Kr}, and I_{Ks} currents were inhibited over multiple pacing rates. It was identified that intracellular Na^{+} and Ca^{2+} concentrations did not depend strongly on I_{Kr} or I_{Ks} inhibition, but that they did depend strongly on both pacing rate and I_{CaL} with and interaction between these dependencies. Consequently, the steady state values of sarcoplasmic Ca^{2+} load and bulk cytosolic Na^{+} were calculated over a grid of combinations of pacing rates and I_{CaL} current inhibition levels, and a polynomial surface depending on these variables were fitted to the concentrations. This was used to estimate the steady state level of ion concentrations before starting new simulations, which reduced the time to reach steady state from minutes to only one or two seconds of simulated time. This greatly increased the efficiency of many practical tasks but did not alter the internal functioning of the model.

References

1. Gandhi NR, Nunn P, Dheda K, Schaaf HS, Zignol M, Van Soolingen D, et al. Tuberculosis 2 multidrug-resistant and extensively drug-resistant tuberculosis: A threat to global control of tuberculosis. Lancet. 2010;375:1830-43.

2. World Health Organization. Global tuberculosis report 2012. 2012.

3. H Gillespie S, Singh K. XDR-TB, what is it; how is it treated; and why is therapeutic failure so high? Recent Patents on Anti-Infective Drug Discovery. 2011;6(2):77-83.

4. Silver LL. Challenges of antibacterial discovery. Clin Microbiol Rev. 2011;24(1):71-109.

5. Kristiansen J, Thomsen V, MARTINS A, Viveiros M, Amaral L. Non-antibiotics reverse resistance of bacteria to antibiotics. In Vivo. 2010;24(5):751-4.

6. Amaral L, Viveiros M. Why thioridazine in combination with antibiotics cures extensively drug-resistant< i> mycobacterium tuberculosis infections. Int J Antimicrob Agents. 2012.

7. Crowle A, Douvas G, May M. Chlorpromazine: A drug potentially useful for treating mycobacterial infections. Chemotherapy. 1992;38(6):410-9.

8. Amaral L, Kristiansen J, Abebe L, Millett W. Inhibition of the respiration of multi-drug resistant clinical isolates of mycobacterium tuberculosis by thioridazine: Potential use for initial therapy of freshly diagnosed tuberculosis. J Antimicrob Chemother. 1996;38(6):1049-53.

9. Bettencourt MV, Bosne-David S, Amaral L. Comparative in vitro activity of phenothiazines against multidrug-resistant mycobacterium tuberculosis. Int J Antimicrob Agents. 2000 Sep;16(1):69-71.

10. Ordway D, Viveiros M, Leandro C, Bettencourt R, Almeida J, Martins M, et al. Clinical concentrations of thioridazine kill intracellular multidrug-resistant mycobacterium tuberculosis. Antimicrob Agents Chemother. 2003;47(3):917-22.

11. Martins M, Viveiros M, Kristiansen JE, Molnar J, Amaral L. The curative activity of thioridazine on mice infected with mycobacterium tuberculosis. In Vivo. 2007;21(5):771-5.

12. van Soolingen D, Hernandez-Pando R, Orozco H, Aguilar D, Magis-Escurra C, Amaral L, et al. The antipsychotic thioridazine shows promising therapeutic activity in a mouse model of multidrug-resistant tuberculosis. PLoS One. 2010;5(9):e12640.

13. Abbate E, Vescovo M, Natiello M, Cufré M, García A, Ambroggi M, et al. Tuberculosis extensamente resistente (XDR-TB) en argentina: Aspectos destacables, epidemiologicos, bacteriologicos, terapeuticos y evolutivos. Revista Argentina de Medicina Respiratoria. 2007;1:19-25.

14. Abbate E, Vescovo M, Natiello M, Cufré M, García A, Montaner PG, et al. Successful alternative treatment of extensively drug-resistant tuberculosis in argentina with a combination of linezolid, moxifloxacin and thioridazine. J Antimicrob Chemother. 2012;67(2):473-7.

15. Kelly HG, Fay J, Laverty S. Thioridazine hydrochloride (mellaril): Its effect on the electrocardiogram and a report of two fatalities with electrocardiographic abnormalities. Can Med Assoc J. 1963;89(11):546.

16. Dessertenne F. La tachycardie ventriculaire a deux foyers opposes variables. Arch Mal Coeur. 1966;59(2):263-72.

17. Fenichel RR, Malik M, Antzelevitch C, Sanguinetti M, Roden DM, Priori SG, et al. Drug-Induced torsades de pointes and implications for drug development. J Cardiovasc Electrophysiol. 2004;15(4):475-95.

18. Belardinelli L, Antzelevitch C, Vos MA. Assessing predictors of drug-induced torsade de pointes. Trends Pharmacol Sci. 2003;24(12):619-25.

19. Yan G, Lankipalli RS, Burke JF, Musco S, Kowey PR. Ventricular repolarization components on the electrocardiogramcellular basis and clinical significance. J Am Coll Cardiol. 2003;42(3):401-9.

20. Kirchhof P, Franz MR, Bardai A, Wilde AM. Giant T–U waves precede torsades de pointes in long QT SyndromeA systematic electrocardiographic analysis in patients with acquired and congenital QT prolongation. J Am Coll Cardiol. 2009;54(2):143-9.

21. Lasser KE, Allen PD, Woolhandler SJ, Himmelstein DU, Wolfe SM, Bor DH. Timing of new black box warnings and withdrawals for prescription medications. JAMA. 2002;287(17):2215-20.

22. Wood AJ, Roden DM. Drug-induced prolongation of the QT interval. N Engl J Med. 2004;350(10):1013-22.

23. Axelsson R, Aspenstrom G. Electrocardiographic changes and serum concentrations in thioridazine-treated patients. J Clin Psychiatry. 1982 Aug;43(8):332-5.

24. Hartigan-Go K, Bateman N, Nyberg G, Mårtensson E, Thomas SHL. Concentration-related pharmacodynamic effects of thioridazine and its metabolites in humans. Clinical Pharmacology & Therapeutics. 1996;60(5):543-53.

25. Reilly J, Ayis S, Ferrier I, Jones S, Thomas S. QTc-interval abnormalities and psychotropic drug therapy in psychiatric patients. The Lancet. 2000;355(9209):1048-52.

26. Harrigan EP, Miceli JJ, Anziano R, Watsky E, Reeves KR, Cutler NR, et al. A randomized evaluation of the effects of six antipsychotic agents on QTc, in the absence and presence of metabolic inhibition. J Clin Psychopharmacol. 2004;24(1):62-9.

27. Salih I, Thanacoody R, McKay G, Thomas S. Comparison of the effects of thioridazine and mesoridazine on the QT interval in healthy adults after single oral doses. Clinical Pharmacology & Therapeutics. 2007;82(5):548-54.

28. Mehtonen OP, Aranko K, Mälkonen L, Vapaatalo H. A survey of sudden death associated with the use of antipsychotic or antidepressant drugs: 49 cases in finland. Acta Psychiatr Scand. 1991;84(1):58-64.

29. Ray WA, Meredith S, Thapa PB, Meador KG, Hall K, Murray KT. Antipsychotics and the risk of sudden cardiac death. Arch Gen Psychiatry. 2001;58(12):1161.

30. Reilly J, Ayis S, Ferrier I, Jones S, Thomas S. Thioridazine and sudden unexplained death in psychiatric in-patients. The British Journal of Psychiatry. 2002;180(6):515-22.

31. Hennessy S, Bilker WB, Knauss JS, Margolis DJ, Kimmel SE, Reynolds RF, et al. Cardiac arrest and ventricular arrhythmia in patients taking antipsychotic drugs: Cohort study using administrative data. BMJ: British Medical Journal. 2002;325(7372):1070.

32. HK Thanacoody R. Thioridazine: The good and the bad. Recent Patents on Anti-Infective Drug Discovery. 2011;6(2):92-8.

33. Redfern W, Carlsson L, Davis A, Lynch W, MacKenzie I, Palethorpe S, et al. Relationships between preclinical cardiac electrophysiology, clinical QT interval prolongation and torsade de pointes for a broad range of drugs: Evidence for a provisional safety margin in drug development. Cardiovasc Res. 2003;58(1):32-45.

34. Haverkamp W, Breithardt G, Camm AJ, Janse MJ, Rosen MR, Antzelevitch C, et al. The potential for QT prolongation and pro-arrhythmia by non-anti-arrhythmic drugs: Clinical and regulatory implications. report on a policy conference of the european society of cardiology. Cardiovasc Res. 2000 Aug;47(2):219-33.

35. Drolet B, Vincent F, Rail J, Chahine M, Deschênes D, Nadeau S, et al. Thioridazine lengthens repolarization of cardiac ventricular myocytes by blocking the delayed rectifier potassium current. J Pharmacol Exp Ther. 1999;288(3):1261-8.

36. Tie H, Walker B, Valenzuela S, Breit S, Campbell T. The heart of psychotropic drug therapy. The Lancet. 2000;355(9217):1825.

37. Milnes JT, Witchel HJ, Leaney JL, Leishman DJ, Hancox JC. hERG K< sup> </sup> channel blockade by the antipsychotic drug thioridazine: An obligatory role for the S6 helix residue F656. Biochem Biophys Res Commun. 2006;351(1):273-80.

38. Antzelevitch C. Heterogeneity of cellular repolarization in LQTS: The role of M cells. European Heart Journal Supplements. 2001;3(suppl K):K2-K16.

39. Yan GX, Antzelevitch C. Cellular basis for the normal T wave and the electrocardiographic manifestations of the long-QT syndrome. Circulation. 1998 Nov 3;98(18):1928-36.

40. Gima K, Rudy Y. Ionic current basis of electrocardiographic waveforms: A model study. Circ Res. 2002 May 3;90(8):889-96.

41. Baumann P, Zullino DF, Eap CB. Enantiomers' potential in psychopharmacology—a critical analysis with special emphasis on the antidepressant escitalopram. European neuropsychopharmacology. 2002;12(5):433-44.

42. Svendsen C, Froimowitz M, Hrbek C, Campbell A, Kula N, Baldessarini R, et al. Receptor affinity, neurochemistry and behavioral characteristics of the enantiomers of thioridazine: Evidence for different stereoselectivities at D_1 and D_2 receptors in rat brain. Neuropharmacology. 1988;27(11):1117-24.

43. Jortani SA, Poklis A. Determination of thioridazine enantiomers in human serum by sequential achiral and chiral high-performance liquid chromatography. J Anal Toxicol. 1993;17(6):374-7.

44. Kristiansen JE, Hendricks O, Delvin T, Butterworth TS, Aagaard L, Christensen JB, et al. Reversal of resistance in microorganisms by help of non-antibiotics. J Antimicrob Chemother. 2007;59(6):1271-9.

45. Hendricks O, Christensen JB, Kristiansen JE. Antibakterielle eigenschaften der phenothiazine. eine behandlungsoption für die zukunft? Chemotherapie Journal. 2004;13(5):203-5.

46. Hendricks O. Antimicrobial effects of selected non-antibiotics on sensitivity and invasion of gram-positive bacteria. Ugeskr Laeger. 2007;169(6):524.

47. Jortani SA, Valentour JC, Poklis A. Thioridazine enantiomers in human tissues. Forensic Sci Int. 1994;64(2):165-70.

48. Glassman AH, Bigger JT. Antipsychotic drugs: Prolonged QTc interval, torsade de pointes, and sudden death. Am J Psychiatry. 2001;158(11):1774-82.

49. Ray WA, Chung CP, Murray KT, Hall K, Stein CM. Atypical antipsychotic drugs and the risk of sudden cardiac death. N Engl J Med. 2009;360(3):225-35.

50. Lu Z, Kamiya K, Opthof T, Yasui K, Kodama I. Density and kinetics of IKr and IKs in guinea pig and rabbit ventricular myocytes explain different efficacy of IKs blockade at high heart rate in guinea pig and rabbit. Circulation. 2001;104(8):951-6.

51. Lengyel C, Iost N, Virág L, Varró A, Lathrop DA, Papp JG. Pharmacological block of the slow component of the outward delayed rectifier current (I_{Ks}) fails to lengthen rabbit ventricular muscle QTc and action potential duration. Br J Pharmacol. 2001;132(1):101-10.

52. Shannon TR, Wang F, Puglisi J, Weber C, Bers DM. A mathematical treatment of integrated ca dynamics within the ventricular myocyte. Biophys J. 2004;87(5):3351-71.

53. Dhein S. Isolated papillary muscles. In: Dhein S, Mohr FW, Delmar M, editors. Practical Methods in Cardiovascular Research. 1st ed. Springer Berlin Heidelberg; 2005. p. 190-7.

54. Fenton FH, Cherry EM. Models of cardiac cell. Scholarpedia. 2008;3(8):1868.

55. Hodgkin AL, Huxley AF. A quantitative description of membrane current and its application to conduction and excitation in nerve. J Physiol. 1952 Aug;117(4):500-44.

56. McAllister RE, Noble D, Tsien RW. Reconstruction of the electrical activity of cardiac purkinje fibres. J Physiol. 1975 Sep;251(1):1-59.

57. Noble D. A modification of the hodgkin--huxley equations applicable to purkinje fibre action and pace-maker potentials. J Physiol. 1962 Feb;160:317-52.

58. Beeler GW, Reuter H. Reconstruction of the action potential of ventricular myocardial fibres. J Physiol. 1977 Jun;268(1):177-210.

59. Luo CH, Rudy Y. A model of the ventricular cardiac action potential. depolarization, repolarization, and their interaction. Circ Res. 1991 Jun;68(6):1501-26.

60. DiFrancesco D, Noble D. A model of cardiac electrical activity incorporating ionic pumps and concentration changes. Philos Trans R Soc Lond B Biol Sci. 1985 Jan 10;307(1133):353-98.

61. Luo CH, Rudy Y. A dynamic model of the cardiac ventricular action potential. I. simulations of ionic currents and concentration changes. Circ Res. 1994 Jun;74(6):1071-96.

62. Zeng J, Laurita KR, Rosenbaum DS, Rudy Y. Two components of the delayed rectifier K^+ current in ventricular myocytes of the guinea pig type. theoretical formulation and their role in repolarization. Circ Res. 1995 Jul;77(1):140-52.

63. Viswanathan PC, Shaw RM, Rudy Y. Effects of IKr and IKs heterogeneity on action potential duration and its rate dependence: A simulation study. Circulation. 1999 May 11;99(18):2466-74.

64. Clancy CE, Rudy Y. Linking a genetic defect to its cellular phenotype in a cardiac arrhythmia. Nature. 1999;400(6744):566-9.

65. Faber GM, Rudy Y. Action potential and contractility changes in $[na^+]_i$ overloaded cardiac myocytes: A simulation study. Biophys J. 2000;78(5):2392-404.

66. Jafri MS, Rice JJ, Winslow RL. Cardiac ca^2 dynamics: The roles of ryanodine receptor adaptation and sarcoplasmic reticulum load. Biophys J. 1998;74(3):1149-68.

67. Winslow RL, Rice J, Jafri S, Marban E, O'Rourke B. Mechanisms of altered excitation-contraction coupling in canine tachycardia-induced heart failure, II: Model studies. Circ Res. 1999 Mar 19;84(5):571-86.

68. Puglisi JL, Bers DM. LabHEART: An interactive computer model of rabbit ventricular myocyte ion channels and ca transport. Am J Physiol Cell Physiol. 2001 Dec;281(6):C2049-60.

Contributions

I: Differential Effects of Thioridazine Enantiomers on Action Potential duration in Rabbit Papillary Muscle

Ask S. Jensen[1], Cristian P. Pennisi[1], Cristian Sevcencu[1], Jørn B. Christensen[2], Jette E. Kristiansen[3], Johannes J. Struijk[1]

[1]Aalborg University, Denmark. [2]University of Copenhagen, Denmark. [3]University of Southern Denmark, Denmark

Published by the European Journal of Pharmacology

II: Model Based Analysis of the Effects of Thioridazine Enantiomers on the Rabbit Papillary Action Potential: Part 1

Ask S. Jensen[1], Cristian P. Pennisi[1], Cristian Sevcencu[1], Jørn B. Christensen[2], Jette E. Kristiansen[3], Johannes J. Struijk[1]

[1]Aalborg University, Denmark. [2]University of Copenhagen, Denmark. [3]University of Southern Denmark, Denmark

Submitted for publication

III: Model Based Analysis of the Effects of Thioridazine Enantiomers on the Rabbit Papillary Action Potential: Part 2

Ask S. Jensen[1], Cristian P. Pennisi[1], Cristian Sevcencu[1], Jørn B. Christensen[2], Jette E. Kristiansen[3], Johannes J. Struijk[1]

[1]Aalborg University, Denmark. [2]University of Copenhagen, Denmark. [3]University of Southern Denmark, Denmark

Submitted for publication

Conclusion

The studies presented in this thesis focus on potential differential effects of the thioridazine enantiomers on cardiac repolarization in the isolated rabbit papillary muscle using transmembrane action potential measurements. It was found that (-)-thioridazine causes significantly less APD prolongation than either (+)-thioridazine or the racemate. This in itself is an indication that (-)-thioridazine may also cause less QT interval prolongation and may have reduced cardiotoxic side effects. However, thioridazine has been reported to have a multitude of effects on ion channels, and indeed the effects observed in the papillary muscles were more complex than a dose-dependent APD prolongation alone. Depending on drug and stimulus frequency, a shortening of the APD also occurred. The specific mechanisms responsible for the observed differences are of great importance to the potential cardiotoxicity of the compounds, and the occurrence of APD shortening also requires further investigation. The mechanisms underlying the observed effects were investigated using computational modeling of the rabbit ventricular papillary electrophysiology.

The action potential is the product of a balance between a number of depolarizing and repolarizing ionic transmembrane currents, which may include voltage gated channels, energy-dependent pumps, and ionic exchangers operating in complex, mutually interacting systems. Consequently, a direct investigation of effects on these mechanisms requires channel-level observations. However, the membrane currents have characteristic effects on the action potential, and therefore, drug exposure may also yield such characteristic effects. By incorporating action potential level observations with a sufficiently descriptive mathematical model of the cellular physiology, it is possible to demonstrate whether a hypothetical mechanism is in agreement with the data, and to make predictions about which mechanisms best match the observations. Due to the multitude of potential effects due to thioridazine, a model-based study based exclusively on action potential recordings cannot provide a comprehensive and accurate description of the effects occurring at the membrane channel level. Instead, the model-based studies presented in this thesis used a simplified model of drug effects to demonstrate that the difference in APD prolongation can plausibly be described by a differential blockade of the I_{Kr} current. This indicates that there is good reason to believe that the differential effect on APD is also associated with a difference in cardiotoxicity.

The results do not provide conclusive evidence that (-)-thioridazine is less likely to cause ventricular arrhythmia than (+)-thioridazine or the racemate. They do, however, provide the first indication that this may indeed be the case and that further investigation is an urgent and worthwhile endeavor. A number of questions are left unanswered which require further study. Firstly, there is a need to directly investigate the effects of the isolated enantiomers on the level of the individual membrane current through patch clamp studies. This may provide an accurate assessment of differences in affinity for inhibition of both I_{Kr} and other currents. Secondly, it is necessary to investigate the effects of the isolated enantiomers on the corrected QT interval in humans, as this is by far the best established and most widely used surrogate measure of proarrhythmic risk, and because it is a requirement in the regulatory process. However, the corrected QT interval is indeed a surrogate measure which has been the subject of great deal of controversy, as some drugs cause substantial QT prolongation but are not proarrhythmic, or are less proarrhythmic than drugs which cause less QT prolongation. I_{Kr} inhibition and risk of Torsades de Pointes is associated with several types of morphological T wave changes, and recent

studies have demonstrated that scoring of T wave morphology changes provides a more reliable indicator of arrhythmic risk. Consequently, a better indication of potential differences in cardiotoxicity may be obtained by investigating not only the effects of the isolated thioridazine enantiomers on corrected QT interval prolongation, but also on changes of T wave morphology scores.

There is an urgent need for progress in the fight against the global problem of increasing antimicrobial drug-resistance, as previously curable diseases are becoming increasingly difficult to treat in many parts of the world. The primary reason for the unnecessarily rapid rate development of antibiotic resistance is incorrect use of antibiotics. Exposure to an antibiotic agent produces a selection pressure which preferentially allows certain microbial strains to further proliferate. Excessive, preemptive, and unnecessary usage of antibiotics serves to drastically increase this selection pressure, and incomplete treatment and addition of new drugs to failing regimens allow resistant strains to survive and develop resistance to an increasing number of compounds. It is clear that the current rate of development of new antibiotics is too slow to effectively reverse this tide of increasing drug-resistance. The first line of defense must be guidelines which promote prudent, careful, and thorough application of antimicrobial treatment. However, counteracting the proliferation of drug-resistance is a slow and difficult process which requires control of antimicrobial treatment on a global scale. For these reasons there is a need for focus on new approaches to combat currently existing and future multi-drug resistant strains. The development of helper compounds that reverse antimicrobial resistance shows great promise and may become an important new tool in such efforts. Thioridazine is particularly interesting in this regard. However, it is also a well-known compound which has been extensively used in the past, and which has cardiotoxic side effects that have already caused the drug to be withdrawn. Consequently, there is much skepticism, both towards the use of an antipsychotic drug in any other role than that of antipsychotic treatment, but also towards the reintroduction of a drug which has already been found to not live up to the current standards of cardiac safety.

The outcomes of this thesis pose new questions, but they have substantial potential implications for addressing safety concerns and for the prospects of introduction of isolated (-)-thioridazine in antimicrobial treatment. This represents the first step towards full determination of the cardiotoxicity of the isolated thioridazine enantiomers. If further studies confirm that (-)-thioridazine does indeed have reduced affinity for blockade of I_{Kr} and that it causes reduced QT interval prolongation and T wave morphology alterations, this will demonstrate that (-)-thioridazine is very likely to be safer treatment than the racemate. In such case, a substantial obstacle on the path to approval of the isolated (-)-thioridazine enantiomer for antimicrobial treatments will be removed. The result may be the introduction of a new effective tool in the treatment of drug-resistant microbial disease.